UNIVERSIDAD NACIONAL DE COLOMBIA
SEDE MEDELLÍN
FACULTAD DE MINAS

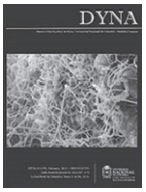

DYNA
http://dyna.medellin.unal.edu.co/

Sol-gel synthesis of zinc oxide nanoparticle at three different temperatures and its characterization via XRD, IR and EPR

Manuel Acosta-Humánez [a], Luis Montes-Vides [b] & Ovidio Almanza-Montero [c*]

[a] *Departamento de Física. Universidad Nacional de Colombia. Bogotá. Colombia. mafacostahu@unal.edu.co*
[b] *Departamento de Geociencias. Universidad Nacional de Colombia. Bogotá. Colombia. lamontesv@unal.edu.co*
[c] *Departamento de Física. Universidad Nacional de Colombia. Bogotá. Colombia. oaalmanzam@unal.edu.co*

Received: May 25th, 2015. Received in revised form: September 11th, 2015. Accepted: September 21th, 2015.

Abstract
In this work, nanoparticles of zinc oxide were synthesized; they were formed using the sol-gel method (citrate route) at calcination temperatures (Tc) of 500, 550 and 600 °C. For all samples studied, IR spectroscopy showed the presence of the bands associated with water molecules present in the zinc oxide and carbon dioxide adsorbed on its surface. The formation of zinc oxide phase was confirmed by XRD, which showed that from 500 ºC it had this type of Wurtzite structure. However, samples calcinated at 600 ºC have higher crystallinity. Crystallite size was calculated using the Scherrer equation. The Rietveld method was used to obtain lattice parameters a and c for Wurtzite cell types as well as cell volume and the ratio c/a of each sample. These parameters do not show significant changes when they are compared with values obtained from samples with different calcination temperatures. Electron paramagnetic resonance showed the presence of defects in the zinc oxide. Three signals with g values of 1.96, 2.00 and 2.04 were associated with oxygen and zinc vacancies. Defects in the structure disappear when the calcination temperature is increased. The sample that was highlighted with the highest concentration of vacancies has a mean crystallite size greater than 30 nm, and this may also be responsible for this feature.

Keywords: X-Ray diffraction, IR spectroscopy, sol-gel method, electron paramagnetic resonance, zinc oxide.

Síntesis sol-gel de nanopartículas de óxido de zinc a tres termperaturas diferentes y su caracterización vía XRD, IR y EPR

Resumen
Se sinterizaron nanopartículas de óxido de zinc (ZnO) mediante el método sol-gel (ruta citrato) a las temperaturas de calcinación (Tc) de 500, 550 y 600 °C.Se mostró por espectroscopía IR la presencia de las bandas asociadas a moléculas de agua presentes en el óxido de zinc así como de dióxido de carbono adsorbido en su superficie, para todas las muestras estudiadas. La tenencia de una estructura tipo wurtzita, propia del ZnO, incluso para las muestras calcinadas a 500 ºC, fue confirmada por XRD, Las muestras preparadas a Tc de 600 ºC tienen mayor cristalinidad que las muestras calcinadas a 500 ºC. El tamaño de cristal fue evaluado por la ecuación de Scherrer. El método Rietveld fue usado para obtener los parámetros de red a y c para la celda tipo wurtzita, así como el volumen de celda y la relación c/a de cada muestra. Estos parámetros no muestran desviaciones significativas cuando ellos son comparados entre valores obtenidos para muestras con distintas temperaturas de calcinación. Por resonancia paramagnética electrónica se mostró la presencia de defectos en el óxido de zinc. Tres señales, con valores de g = 1.96, 2.00 y 2.04 fueron asociados a vacancia de oxígenos y vacancias de Zinc respectivamente. Los defectos en la estructura desaparecen a medida que se incrementa la temperatura de calcinación. La muestra con la mayor concentración de vacancias tiene un tamaño medio de cristalito mayor de 30 nm y esto último puede ser el responsable de esta característica.

Palabras clave: Difracción de rayos X, espectroscopía IR, método sol-gel, resonancia paramagnética electrónica, ZnO.

1. Introduction

Zinc oxide (ZnO) is a type II-VI semiconductor with a direct band gap of 3.37 eV and stable Wurtzite type structure with lattice parameters a = 3.25 Å and c = 5.21 Å [1]. It is an important semiconductor material due to its applications, which include transparent conductive oxides (TCO) [2,3], ultraviolet (UV) blockers, and photocatalysts, among others. As photocatalysts, the

reduction of organic pollutant compounds and the remediation of organic contaminants, mainly azo type (compounds that interact with visible light), can be mentioned as being the most important in terms of usefulness. The presence of free radicals or vacancies in them are responsible for these applications and some authors have established that the amount of them is dependent on the crystal size, given that the ratio surface / volume increases as the size of the material decreases to a nanometer range [4,5]. ZnO is a relatively open structure with a hexagonal-close-packed lattice where Zn atoms occupy half of the tetrahedral sites, while all octahedral sites are empty [6]. The open structure also influences the nature of defects and the diffusion mechanism. The identity, quantity, and stability of these radicals or vacancies are features to consider when this material is required in a particular application. Applications for these types of materials depend on their electrical and magnetic properties and these depend on the method by which they were prepared [1-5].

Many methods for the production of ZnO nanostructures have been described in the literature such as laser ablation [7], hydrothermal methods [8], electrochemical depositions [9], chemical vapor deposition [10], thermal decomposition [11], the combustion method [12] and the co-precipitation method [13,14], resulting in zinc oxide nanoparticles with a nanometric size. The sol-gel method allows the mixture of the initial reagent on an atomic level, which, while there is control of chemical composition and there are quite homogeneous materials in its composition, reduces the possibility of having impurities that are difficult to detect and has good reproducibility. Materials of high surface area can be prepared at a low cost and the experimental procedure can be easily undertaken [15,16]. In this work, pure zinc oxide was synthesized using the sol-gel method (citrate route) at various calcination temperatures. Structural properties and the mean crystal size were determined by XRD, and its purity was assessed by infrared spectroscopy. The presence of free radicals, vacancies or defects was observed by electron paramagnetic resonance, which could be associated to potential uses of these materials as reductors of organic pollutant compounds.

2. Materials and methods

Nanoparticles of Zinc oxide were prepared by the sol-gel (citrate route) method using Zinc Nitrate, $Zn(NO_3)_2 \bullet 6H_2O$ (Panreac) as the starting materials. Citric acid $C_6H_8O_7 \bullet H_2O$ (Panreac) was used as a complexing agent. A stoichiometric weight of metallic cation was homogeneously mixed in deionized water using magnetic stirring at 70 °C. Then, Citric acid was also dissolved in deionized water for 30 minutes. The Citrate/Nitrate ratio used was 1. The solution of Zinc Nitrate in the solution of Citric acid was added slowly. The reaction mixture was heated at 70 °C with continuous stirring until gel formation. The product obtained was dried at 130 °C for 12 hours and pulverized for 30 minutes using an agate mortar. The precursor materials were calcined at the calcination temperature (Tc) of 500, 550 and 600 °C for 12 hours [4]. These samples were denominated in ZnOTc form. The reaction of zinc oxide formation can be written as described in equation (1):

$$Zn(NO_3)_2 \cdot 6H_2O + C_6H_8O_7 \cdot H_2O + 4O_2 \rightarrow ZnO + 2NO_2 + 6CO_2 + 11H_2O \quad (1)$$

Infrared spectra were carried out in a Fourier transform spectrophotometer Shimadzu IRAffinity-1 in the range of wavenumber 4000-600 cm^{-1}. X-ray diffraction measurements were performed on a diffractometer Panalytical Pro MPD using polycrystalline silicon as a calibration standard in 2θ range of 10-90, and using CuKα1 radiation and a step size (2θ) of 0.0260. Sweep time was 18.6860 s. The EPR spectra were carried out on a Bruker X-band spectrometer ESP-300 at different temperatures. A frequency of 9.45 GHz and a modulation amplitude of 10.496 G were also used in this procedure.

3. Results and discussion

The purity and molecular structure of the samples were determined by infrared spectroscopy. Fig. 1 shows the FTIR spectra of the nanocrystalline powders of zinc oxide. The two peaks at ~3428 and 1590 cm^{-1} are attributed to the stretching vibrations of the -OH group and the deformation of H-O-H bond, which are associated with small amounts of water existing in the zinc oxide [1]. The band corresponding to ~ 2400 cm^{-1} is associated with CO_2 molecules that are adsorbed on the surface of ZnO [17,18]. The bands that are near to 1000 cm^{-1} are associated with metal-Oxygen tension and bending, in this case, Zn-O. An increase of the temperature in this band is associated with high Zn-O bonding due to thermal evolution of samples [18]. Two small bands are observed at 2920 and 2850 cm^{-1}, possibly due to $-CH_2$ groups belonging to the metal-organic chain formed during synthesis [18]; these are small residues and the bands are not intense. All these results were independent of calcination temperature (Tc).

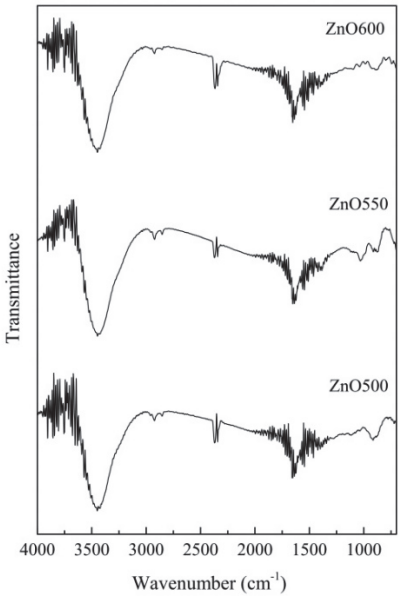

Figure 1. Infrared spectra for Zinc oxide samples at different Tc values. Source: The authors.

Fig. 2 shows diffractograms for ZnO samples as well as the precursor material studied at different calcinations temperatures. At this point, the evolution of the precursor material is displayed, which is an organometallic compound (zinc citrate), and its evolution towards zinc oxide can be appreciated when calcination temperature is higher than 500 ºC. For all samples studied, all diffraction peaks were associated with Zinc oxide according to the PDF-Card 36-1451 (2004 PDF2 database) and the structure was a wurtzite type. There were no observed peaks corresponding to some of the reagent precursors or other secondary phases, and all samples have good crystallinity, which increases at the same time as the calcination temperature Tc. The Wurtzite structure for ZnO, is therefore observed from Tc = 500 ºC and this calcination temperature could be enough to obtain samples that are going to be used as a photocatalyst, that in turn decreasing production costs.

It is worthwhile mentioning that the diffraction peak associated with the plane (101) is the most intense one, and this may be due to the synthesis method used since it has been reported that for thin films the most intense level corresponds to the (002) reflection [19-21]. The preferred orientation of growth, determined using a texture coefficient TC (hkl) was calculated using equation (2) [19] and showed that for all samples calcinated, the preferred growth plane was (100) except ZnO calcinated at 600 °C, which grew preferentially in the plane direction (101).

$$TC(hkl) = \frac{I(hkl)/I_0(hkl)}{N^{-1}\sum_n I(hkl)/I_0(hkl)} \qquad (2)$$

In this equation, *I (hkl)* is the measured relative intensity of the plane *(hkl), I_0 (hkl)* is the relative intensity of the standard plane *(hkl)* taken from the JCPDS database, N is the number of reflections in the diffractogram, 7 being the most intense (Fig. 2), and *n* is the number of used diffraction peaks, which in our case was 3 associated with the planes (100), (002) and (101). For a sample that has randomly oriented crystallites, the value of *TC(hkl)* is equal to 1, whereas if this value increases, it means that the greater abundance of crystals is oriented in one particular direction *(hkl)* [20] . *TC(hkl)* data for the three main diffraction peaks (100), (002) and (101) are shown in Table 1.

Mean crystallite size was estimated from the Scherrer equation, with a gaussian fit,

$$D_s = \frac{K\,\lambda}{\beta\cos\theta} \qquad (3)$$

where β is integral breadth (in radians), λ is the wavelength of X rays (CuK_α radiation, 0.1540598 *nm*), *K* is Scherrer's constant that depends on the directions of the crystal lattice and crystal morphology [21]; its value is 0.94 and θ is Bragg's angle. Integral breadths of diffraction peaks for all samples were calculated using the following equation:

$$\beta = [(\beta_m)^2 - (\beta_{instr})^2]^{1/2} \qquad (4)$$

Where β_{instr} is the integral breadth for a calibration standard, and β_m the integral breadth for diffraction peaks of synthesized samples. The results for D_s are shown in Table 2, and D_s values are nanometric. The lowest D_s is obtained when calcination temperature is 550 °C; ZnO calcinated at 500 °C has an average crystallite size above 30 nm. Differences in crystal sizes (Ds) are determined by the Scherrer equation, and this is true for all samples as they have different integral breadth values as consequence of the fact they were calcinated at different temperature Tc.

The lattice parameters a and c as well as cell volume (V) were calculated by the Rietveld method, using the Fullprof program [22]. Table 2 shows the calculated values. a and c do not change significantly with calcination temperature. The ratio c/a shows the deviation that crystalline structure of the samples presented with respect to the theoretical network hcp (hexagonal compact packing, the value of which is 1.633). The deviations regarding the theoretical value may be products of microstrains and the concentration of defects in the crystal.

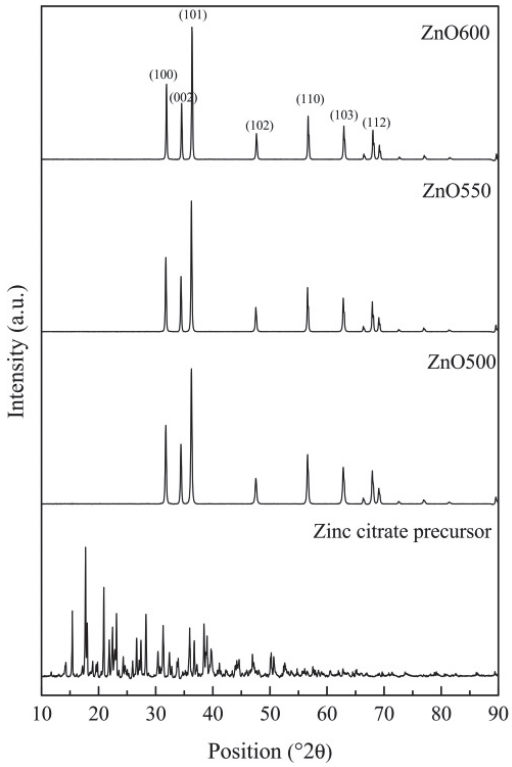

Figure 2. Diffractograms of ZnO, including precursor material, at different Tc values.
Source: The authors.

Table 1.
TC (hkl) values calculated from equation (2).

	Planes		
	(100)	**(002)**	**(101)**
Samples		***TC (hkl)***	
ZnO500	2.370	2.341	2.289
ZnO550	2.376	2.335	2.289
ZnO600	2.314	2.289	2.398

Source: The authors.

Table 2.
Mean crystallite size is given by the Scherrer equation (D_s). Cell parameters a and c for a hexagonal cell, cell volume V and c/a axial ratio are also shown in the table.

Samples	D_S (nm)	a (Å)	c (Å)	V (Å^3)	c/a
ZnO500	30.9	3.2509	5.2090	47.675	1.6023
ZnO550	18.0	3.2507	5.2081	47.661	1.6022
ZnO600	21.9	3.2516	5.2093	47.699	1.6021

Source: The autors.

Fig. 3 shows the EPR spectra for the Zinc oxide samples that are calcinated at three different temperatures. At T_c = 500 ° C three signals are observed having g values of 1.96, 2.00 and 2.04. Some authors have associated these lines to defects in Zinc oxide [4]. The signal localized at the g = 1.96 line was attributed to Oxygen vacancies [4,23,24]. The other two lines are associated with Zinc vacancies [25]. Stehr *et al.* attributed these lines to shallow donors, which show a slight anisotropy because of the Wurtzite type crystal structure of zinc oxide [26]. The sample calcinated at 550 °C showed a small concentration of defects associated with Oxygen vacancies, while the sample calcinated at 600 ° C showed no vacancies, at least in the order of determination of these defects by EPR. It means that pure ZnO calcinated at 550 ºC could be used as a photocatalyst if the oxidation/reduction activity were caused by the presence of defects or vacancies. The sample is highlighted with the highest concentration of vacancies that has a mean crystallite size greater than 30 nm, and this may also be responsible for this feature.

4. Conclusion

Zinc oxide nanoparticles were synthesized at calcination temperatures of 500, 550 and 600 °C. For all samples, the formation of wurtzite-type structures of zinc oxide was observed. The crystal size indicates that samples contain nanosized crystals, and that there are also small microstrains associated with small variations in the hexagonal lattice of zinc oxide. Lattice parameters showed no significant variations in the unit cell due to variation of the calcination temperature. The presence of water and Carbon dioxide molecules on the surface of zinc oxide was evidenced by infrared spectroscopy. Zinc vacancies and oxygen were shown by electron paramagnetic resonance, a process in which their disappearance is shown as long as the calcination temperature increases. The presence of vacancies in samples calcined at Tc = 500 °C, which reacts with a mean crystallite size above 30 nm should be the best catalyst performance or oxidizing/reducing agent.

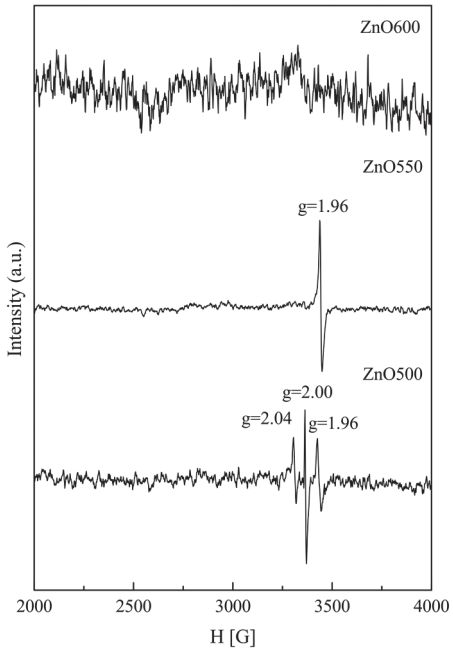

Figure 3. EPR spectra for zinc oxide samples at different Tc values.
Source: The authors.

Acknowledgment

We would like to give thanks to the DIB of the National University of Colombia for their financial support through project 15848. Additionally, we thank professor Mario Barrera for facilitating our use of the equipment and laboratories for the material synthesis.

References

[1] Jagannatha-Reddy, A., Kokila, M.K, Nagabhushana, H., Chakradhar, R.P.S, Shivakumara, C., Rao J.L. and Nagabhushana, B.M., Structural, optical and EPR studies on ZnO:Cu nanopowders prepared via low temperature solution combustion synthesis. J. Alloys. Compd. 509(17), pp. 5349-5355, 2001. DOI: 10.1016/j.jallcom.2011.02.043

[2] Hisono, H., Recent progress in transparent oxide semiconductors: Materials and device application. Thin Solid Films. 515(5), pp. 6000-6014, 2007. DOI: 10.1016/j.tsf.2006.12.125

[3] Becheri, A., Durr, M., Lo Nostro, P. and Baglioni, P., Synthesis and characterization of zinc oxide nanoparticles: Application to textiles as UV absorbers. J. Nanopart. Res. 10, pp. 679-689, 2008. DOI: 10.1007/s11051-007-9318-3

[4] Acosta-Humánez, F., Cogollo-Pitalúa, R. and Almanza, O., Electron paramagnetic resonance in $Zn_{1-x}Co_xO$. J. Magn. Magn. Mater. 329, pp. 39-42, 2013. DOI: 10.1016/j.jmmm.2012.10.026

[5] Wu, C., Shen, L., Shang, Y.C. and Huang, Q., Solvothermal synthesis of Cr-doped ZnO nanowires with visible light-driven photocatalytic activity. Mat. Lett. 65(12), pp. 1794-1796, 2011. DOI: 10.1016/j.matlet.2011.03.070

[6] Cao, B., Gong, H., Zeng, H. and Cai, W.P. Photoluminiscence / Fluorescence spectroscopic technique for nanomaterials characterization, in Nanomaterials: Processing and characterization with lasers, Weinheim, Wiley, 2012, pp. 597-616.

[7] Scarisoreanu, N., Metai, D.G., Dinescu, G, Epurescu, G, Ghica, C, Nistor, L.C. and Dinescu, M., Properties of ZnO thin films prepared by radio-frequency plasma beam assisted laser ablation. Appl. Surf. Sci. 247, pp.518-525, 2005. DOI: 10.1016/j.apsusc.2005.01.140

[8] Ni, Y.H., Wei, X.W., Hong, J.M. and Ye, Y., Hydrothermal synthesis and optical properties of ZnO nanorods. Mater. Sci. Eng., B, 121, pp. 42-47, 2005. DOI: 10.1016/j.mseb.2005.02.065

[9] Chang, S., Yoon, S.O., Park, H.J. and Sakai, A., Luminescence properties of Zn nanowires prepared by electrochemical etching. Mater. Lett. 53, pp. 432-436, 2002. DOI: 10.1016/S0167-577X(01)00521-3

[10] Wu, J.J. and Liu, S.C., Low-temperature growth of well-aligned ZnO nanorods by chemical vapor deposition. Adv. Mater. 14, pp. 215-218, 2002. DOI: 10.1002/1521-4095(20020205)14:3<215::AID-ADMA215>3.0.CO;2-J

[11] Wang, R.C. and Tsai, C.C., Efficient synthesis of ZnO nanoparticles, nanowalls, and nanowires by thermal decomposition of zinc acetate at a

low temperature. Appl. Phys. A. 94, pp. 241-245, 2009. DOI 10.1007/s00339-008-4755-0
[12] Lamas, D.G., Lascalea, G.E. and Walsoc, N.E., Synthesis and characterization of nanocrystalline powders for partially stabilized zirconia ceramics. J. Eur. Ceram. Soc. 18, pp. 1217-1221, 1998. DOI: 10.1016/S0955-2219(98)00045-4
[13] Kumar, S.S., Venkateswarlu, P., Rao, V.R. and Rao, V.R., Synthesis, characterization and optical properties of zinc oxide nanoparticles. Int. Nano Lett [Online]. 30(3), pp. 2-6, 2013. [Date of reference 11th October of 2015]. Available at: http://www.inl-journal.com/content/pdf/2228-5326-3-30.pdf
[14] Ruiz, C.V. and Rodríguez-Páez, J.E., Aluminatos de sodio obtenidos del sistema $Al(NO_3)_3{\cdot}9H_2O$ a través del método de precipitación controlada. Ingeniería e Investigación [Online]. 30(2), pp. 16-24, 2010. [Date of reference 13th October of 2015]. Available at: http://www.revistas.unal.edu.co/index.php/ingeinv/article/view/15726/34068
[15] Jokela, S.J. and McCluskey, M.D., Structure and stability of O-H donors in ZnO from high-pressure and infrared spectroscopy. Phys. Rev. B. 72(11), pp. 113201(1-4), 2005. DOI: 10.1103/PhysRevB.72.113201
[16] Montenegro-Hernández, A. y Rodríguez-Páez, J.E., Síntesis óxido de estaño altamente reactivo utilizando como precursor etilhexanoato de estaño. Ingeniería e Investigación [Online]. 29(1), pp. 47-52, 2009 [Date of reference 13th October of 2015] Available at: http://www.revistas.unal.edu.co/index.php/ingeinv/article/view/15142/34413.
[17] Nejati, K., Rezvani, Z. and Pakizevand, R., Synthesis of ZnO nanoparticles and investigation of the ionic template effect on their size and shape. Int. Nano Lett. [Online]. 1, pp. 75-81, 2011 [date of reference December 15th of 2014]. Available at: http://inljournal.com/?_action=article&vol=1&issue=4&_is=Volume+1%2C+Number+2+%28July+2011%29
[18] Nakamoto, K., Infrared and raman spectra of inorganic and coordination compounds, Applications in coordination, organometallic, and bioinorganic chemistry. Wiley, New York, 2009.
[19] Caglar, Y., Sol-gel derived nanostructure undoped and cobalt doped ZnO: Structural, optical and electrical studies J. Alloys Compd. 560, pp. 181-188, 2013. DOI: 10.1016/j.jallcom.2013.01.080
[20] Xu, C., Cao, L., Su, G., Liu, W., Qu, X. and Yu, Y., Preparation, characterization and photocatalytic activity of Co-doped ZnO powders. J. Alloys Compd. 497(1-2), pp. 373-376, 2010. DOI: 10.1016/j.jallcom.2010.03.076
[21] Yang, J.H, Zhao, L.Y., Ding, X., Yang, L.L., Zhang, Y.J., Wang, Y. X. and Liu, H.L., Magnetic properties of Co-doped ZnO prepared by sol-gel method. Materials Science and Engineering B., 162(3), pp. 143-146, 2009. DOI: 10.1016/j.mseb.2009.03.020
[22] Rodríguez-Carvajal, J., Fullprof suite software: Crystallographic tools for rietveld, profile matching and integrated intensity refinements for X-ray and/or neutron data. Version 5.30. Laboratorie Leon, Brillounin, Gifsuryvette, France, 2012.
[23] Vlasenko, L.S., Magnetic resonance studies of intrinsic defects in ZnO: Oxygen vacancy. Appl Magn Reson. 39(1), pp. 103-111, 2010. DOI: 10.1007/s00723-010-0140-1
[24] Janotti, A. and Van de Walle, C.G., Native point defects in ZnO. Phys. Rev. B. 76(16), pp. 165202(22), 2007. DOI: 10.1103/PhysRevB.76.165202
[25] Vlasenko, L.S. and Watkins, G.D., Optical detection of electron paramagnetic resonance for intrinsic defects produced in ZnO by 2.5-MeV electron irradiation in situ at 4.2 K. Phys. Rev. B. 72(3), pp. 035203(12), 2005. DOI: 10.1103/PhysRevB.72.035203
[26] Stehr, J.E., Meyer, B.K. and Hofmann, D.M., Magnetic resonance of impurities, intrinsic defects and dopants in ZnO. Appl Magn Reson. 39(1), pp. 137-150, 2010. DOI: 10.1007/s00723-010-0142-z

M. Acosta-Humánez, received his BSc. in Chemistry in 2009 from the Universidad de Córdoba, Montería, Colombia. In 2015 he received and MSc. Eng. Degree in Materials and Processes from the Universidad Nacional de Colombia, Bogotá, Colombia. His research interests include: Chemical synthesis process of inorganic materials (oxides), characterization techniques (XRD, EPR, IR, UV-vis) as well as electrochemical methods for materials synthesis and characterization.
ORCID: 0000-0003-0610-4831.

L. Montes-Vides, received his BSc. in Physicist - graduated from the Universidad Nacional de Colombia, MSc. in Engineering in 1987, from the Universidad Nacional de Colombia, and Dr. in Science – Geophysics in 1998. from the Universidade Federal do Pará, Brazil. He has worked at the Universidad Nacional de Colombia in Bogotá since 1990 as a lecturer on the following programs: undergraduate program in Geology, graduate programs in MSc. Geophysics and Doctorate program in Geosciences, all from the Faculty of Sciences. His research areas focus on Seismic prospecting, seismic inversion, seismic modeling and applied computing mathematics. He is a reviewer of the following scientific journals: ESRJ, Revista da SBGf, J.Appl. Geophysics and CT&F.
ORCID: 0000-0002-7470-9202

O. Almanza-Montero, received his PhD. in Physics in 2000, from the Universidad de Valladolid, Spain, and his MSc. in Physics from the Universidad Nacional de Colombia. He is currently a professor in this University and has worked there since 1996. His research is focused on Materials science such as semiconductor and antioxidant activity of Colombian fruits. He is author of more than 50 papers published in different journals. He regularly uses the following characterization techniques: (XRD, EPR, IR, UV-vis).
ORCID: 0000-0002-5141-6079